Journal of Coordination Chemistry

ISSN: 0095-8972 (Print) 1029-0389 (Online) Journal homepage: http://www.tandfonline.com/loi/gcoo20

Synthesis, spectroscopic characterization, antimicrobial activity and crystal structure of silver and copper complexes of sulfamethazine

Sanjay M. Tailor & Urmila H. Patel

To cite this article: Sanjay M. Tailor & Urmila H. Patel (2015) Synthesis, spectroscopic characterization, antimicrobial activity and crystal structure of silver and copper complexes of sulfamethazine, Journal of Coordination Chemistry, 68:13, 2192-2207, DOI: 10.1080/00958972.2015.1055258

To link to this article: http://dx.doi.org/10.1080/00958972.2015.1055258

Journal of Coordination Chemistry, 2015
Vol. 68, No. 13, 2192–2207, http://dx.doi.org/10.1080/00958972.2015.1055258

Synthesis, spectroscopic characterization, antimicrobial activity and crystal structure of silver and copper complexes of sulfamethazine

SANJAY M. TAILOR* and URMILA H. PATEL

X-ray Crystallography Laboratory, Department of Physics, Sardar Patel University, Anand, India

(*Received 7 November 2014; accepted 9 April 2015*)

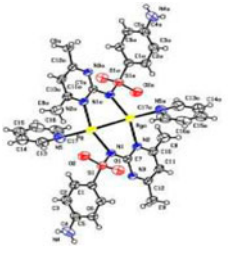

[Ag(smz)(pyridine)] **(I)**

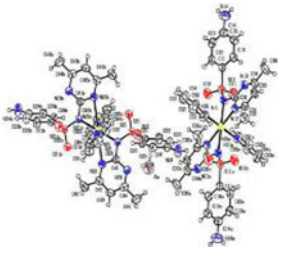

[Cu(smz)$_2$(pyridine)$_2$] (H_2O) **(II)**

Two new transition metal (Ag and Cu) complexes of sulfamethazine with different stoichiometries and coordination environments are synthesized, characterized, and tested as antimicrobial agents.

Silver(I) and copper(II) complexes of 4-amino-N-(4,6-dimethyl-2-pyrimidinyl) benzenesulfonamide (smz) have been synthesized and characterized by elemental analysis and infrared (IR), ^{1}H NMR, and UV–vis spectroscopy. [Ag(smz)(pyridine)] (**1**) crystallizes in monoclinic system with space group $P2_1/c$ and $Z = 4$, while [Cu(smz)$_2$(pyridine)$_2$]·H_2O (**2**) crystallizes in triclinic system with space group *P-1* and $Z = 2$. X-ray analysis revealed that silver in **1** is four-coordinate exhibiting distorted tetrahedral geometry, while copper in **2** is coordinated to six nitrogens leading to a highly distorted octahedral geometry. The molecular structures of both **1** and **2** are stabilized by N–H···O and C–H···π intermolecular and C–H···O intramolecular interactions. Water plays a significant role in crystal packing by forming strong N–H···O_{water} intramolecular as well as O_{water}–H···N intermolecular interactions in **2**. The results of IR, UV–vis, ^{1}H NMR spectral data and thermal analysis for **1** and **2** suggest that the binding of silver and copper to the sulfonamidic nitrogen is in agreement with the crystal structure determination. Antimicrobial activities of silver (**1**) and copper (**2**) complexes of sulfamethazine are studied by the dilution method against *Staphylococcus aureus* and *Escherichia coli* strains.

Keywords: Ag and Cu complexes; Sulfamethazine; Spectroscopic analysis; Crystal structure; Thermogravimetric study; Antimicrobial activity

*Corresponding author. Email: sanjay_tailor10@yahoo.com

1. Introduction

Sulfonamides were the first effective chemotherapeutic agents to be employed systematically for the prevention and cure of bacterial infection in human beings. Sulfonamide derivatives through exchanges of functional groups without modification of the structural S $(O)_2N(H)$ feature can exhibit a wide variety of pharmacological activities, such as antidiabetic, antibacterial, and antitumor [1–4]. Metal complexes of sulfonamides have received interest in bioinorganic chemistry [5–9] as sulfonamides are a vital class of antimicrobial agents in the world owing to their low cost and ability to slow bacterial growth in wounds or infected organs without appreciable toxicity to normal tissues. For example, a Ag(I)–sulfadiazine complex is used for human burn treatment [6, 7] and the Zn(II)–sulfadiazine complex is used for prevention of bacterial infection in burned animals [8, 9]. Since the number of synthesized metal complexes of antibiotic sulfa drugs has increased, the interaction of metal ions with drugs administered for therapeutic reasons has become a subject of importance.

Sulfamethazine (4-amino-N-(4,6-dimethyl-2-pyrimidinyl)benzenesulfonamide, smz) is one of the constituents of the triple sulfa drugs, clinically used in veterinary medicine as an antibacterial compound to treat gastrointestinal and respiratory tract infections [10]. Thus, sulfamethazine compounds are widely used for their bactericidal action and single-crystal X-ray structures of many of them have been solved [11, 12]. Our interest has focused on the synthesis and characterization of metal complexes bearing sulfonamide ligands. Heterocyclic compounds with both sulfur and nitrogen in the ring system have frequently been used in the synthesis of biologically active complexes. Biological activity gets enhanced on undergoing complexation with metals [13, 14]. Several sulfonamide metal complexes showed higher activity than free ligand [15–17].

Sulfamethazine is a sulfa-based drug, used as an antibacterial agent to treat diseases [10], containing several groups with donors to interact with metal ions: Ar–NH_2, NH sulfonamide, SO_2–R, and N heterocyclic atoms (figure 1). Sulfamethazine can act as a bidentate ligand. Binuclear $[Cu_2(CH_3COO)_2(smz)_2]\cdot 2DMF$ and polymeric $\{[Cu(smz)_2]\cdot 2H_2O\}_\infty$ have been isolated, characterized, and their magnetic properties discussed by Borras *et al.* [18]. Recently, the crystal structures of octahedral Cu(II) [19], Zn(II), and Cd(II) sulfamethazine [20] complexes, prepared from the acid form in presence of ammonia as a deprotonating agent, showed an important aspect in which the coordination sphere is formed from pyrimidine, and sulfonamidic nitrogen of two sulfa ligands, water, and the terminal amino of a third sulfa ligand. Single-crystal X-ray structure of the mercury complex of sulfamethazine

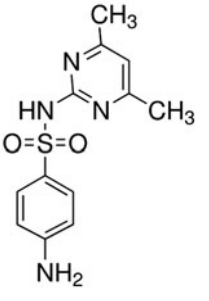

Figure 1. Formula of sulfamethazine (smz).

$[Hg(smz)_2(DMF)_2]$ was reported by Hossain *et al.* [21], but the crystal structure of silver complex of sulfamethazine has not been determined.

In this article, the synthesis and characterization of silver and copper complexes of sulfamethazine are described and their crystal structures are determined.

2. Experimental

2.1. *Chemicals*

Sodium sulfamethazine (Sigma, >99%), silver nitrate, copper acetate, and all other reagents are of the highest grade commercially available and used without purification.

2.2. *Instruments*

Elemental analyses (C, H, and N) are carried out using a Perkin Elmer 2400-II CHN elemental analyzer. Infrared (IR) spectra are recorded on a Perkin Elmer FT-IR spectrometer GX spectrum using KBr pellets. UV–vis spectra are recorded on a Shimadzu UV-3600 spectrometer in DMSO. ^{1}H NMR spectra are recorded on a Bruker Avance DPX-200 spectrometer in d_6-DMSO. Thermogravimetric (TG) analysis is carried out in nitrogen using Seiko SII-EXSTAR TG/DTA-7200.

2.3. *Synthesis of the complexes*

2.3.1. Preparation of the silver sulfamethazine complex [Ag-smz]: [Ag(smz)(pyridine)], complex (1). Sodium salt of sulfamethazine (0.6006 g, 2 mmol) is dissolved in hot methanol. To this solution, an aqueous solution of silver nitrate (0.1698 g, 1 mmol) is added with constant stirring and the mixture is refluxed for 3 h. A white precipitate is formed, filtered, and washed with hot distilled water and methanol successively and dried in a desiccator over anhydrous $CaCl_2$. The yield at the end of reaction for the complex is 40%. Elemental analysis results for $[C_{12}H_{13}N_4Ag_1O_2S_1]$: Calcd (%): C, 37.41; H, 3.40; N, 14.54. Found (%): C, 37.10; H, 3.34; N, 13.61.

2.3.2. Preparation of the copper sulfamethazine complex [Cu-smz]: $[Cu(smz)_2(pyridine)_2]\cdot H_2O$ (2). Sodium salt of sulfamethazine (0.6006 g, 2 mmol) is dissolved in hot methanol. To this solution, an aqueous solution of copper acetate (0.1816 g, 1 mmol) is added with constant stirring and the mixture is refluxed for 3 h. A light yellowish precipitate is formed, filtered, and washed with hot distilled water and methanol successively and dried in a desiccator over anhydrous $CaCl_2$. The yield at the end of reaction for the complex is 35%. Elemental analysis results for $[C_{24}H_{28}N_8Cu_1O_5S_2]$: Calcd (%): C, 45.30; H, 4.43; N, 17.61. Found (%): C, 42.19; H, 4.59; N, 15.62.

Complexes **1** and **2** are insoluble in water and in most common solvents but soluble in DMSO, DMF, and pyridine. After several unsuccessful attempts, it was possible to grow a few tiny white crystals of **1** and tiny light yellow crystals of **2** from pyridine solution suitable for X-ray structure analysis.

2.4. *X-ray crystallography*

Crystallographic data are collected on a Bruker Kappa APEX-II CCD diffractometer with graphite monochromated MoKα radiation ($\lambda = 0.71703$ Å) at $T = 296.15$ K. The structures are solved by direct methods with SHELXS-2013 [22] and anisotropic thermal parameters for all non-hydrogen atoms are refined by full-matrix least squares against F^2 with SHELXL-2013 [23]. The hydrogens are positioned geometrically with N–H = 0.90 Å (for NH_2), C–H = 0.96 Å (for CH_3), and C–H = 0.93 Å for aromatic hydrogens. They are constrained to ride on their parent atoms with U_{iso} (H) = 1.2 U_{eq} (carrier atoms of CH, NH) and U_{iso} (H) = 1.5 U_{eq} (carrier atoms of CH_3). PLATON [24] and ORTEP-3 [25] within WinGX [26] are used to prepare materials for publication.

2.5. *Microbiological assays*

Micro broth dilution method is used to determine the minimal inhibitory concentration (MIC) of the antimicrobial agent against gram negative (*Escherichia coli*) and gram positive (*Staphylococcus aureus*) bacteria. The steps for performing the micro broth dilution method are based on recommendations from the National Committee for Clinical Laboratory Standards [27].

The standard strains used are *E. coli* MTCC 422 and *S. aureus* MTCC 96. Mueller Hinton Broth is used as nutrient medium at 37 °C to grow and dilute the drug suspension for the test bacteria. DMSO is used as diluent to get desired concentration of drugs to test on standard bacterial strains. Serial dilutions are prepared in primary and secondary screening. Compound and standard drugs are diluted obtaining 2000 μg mL^{-1} concentration as a stock solution. In primary screening, 1000, 500, and 250 μg mL^{-1} concentrations of the synthesized drugs are taken. The active synthesized compounds in this primary screening are further diluted to obtain 200, 125, 100, 62.5, 50, 25, 12.5, and 6.250 μg mL^{-1} concentrations for secondary screening. Inoculum's size for test strain is adjusted to 10^8 CFU mL^{-1} by comparing the turbidity. MIC is the lowest concentration of a compound in DMSO that exhibited no visual growth of the organisms in the culture tubes. Each of the above experiments is repeated three times along with a control set using DMSO. The mean value obtained for three individual replicates is then used to calculate the growth inhibition zone of each sample.

3. Results and discussion

3.1. *Crystal structure determination*

Suitable single crystals grown by slow evaporation from a pyridine solution of **1** and **2** are used for X-ray crystal structure determination. The single-crystal data and refinement details for [Ag(smz)(pyridine)] (**1**) and [$Cu(smz)_2(pyridine)_2$]·H_2O (**2**) are summarized in table 1. The ORTEP views for **1** and **2** with 50% probability displacement ellipsoids along with atom numbering scheme are depicted in figures 2 and 3, respectively. The selected bond lengths and angles for **1** and **2** are listed in table 2 and the hydrogen bonds are tabulated in table 3.

Table 1. Crystal data and structure refinement for [Ag(smz)(pyridine)] (**1**) and [Cu(smz)$_2$(pyridine)$_2$]·H$_2$O (**2**).

Compound	**1**	**2**
Empirical formula	$C_{17}H_{18}N_5AgO_2S_1$	$C_{34}H_{38}N_{10}CuO_5S_2$
Formula weight	464.3	794.4
Crystal system	Monoclinic	Triclinic
Space group	*P2$_1$/c*	*P-1*
a (Å)	9.8589(3)	11.6180(5)
b (Å)	11.0815(3)	13.0699(6)
c (Å)	17.1298(5)	14.4250(10)
α (°)	90	100.202(3)
β (°)	98.422(2)	104.619(3)
γ (°)	90	114.491(2)
Volume (Å^3)	1851.27(6)	1827.38(42)
Z	4	2
Temperature (K)	296.15	296.15
Calcd density (Mg m^{-3})	1.67	1.44
Absorption coefficient (mm^{-1})	1.223	0.768
F(0 0 0)	936	826
θ range for data collection (°)	2.1–27.5	1.8–27.6
Index ranges	$-12 \le h \le 12$; $-14 \le k \le 14$; $-22 \le l \le 16$	$-15 \le h \le 15$; $-16 \le k \le 16$; $-17 \le l \le 18$
Reflections collected	15,323	29,947
Unique reflections	4249	8435
R_{int}	0.0225	0.0272
Goodness-of-fit on F^2	1.018	1.041
Data/parameters	4249/235	8435/474
Final *R* indices [$I \ge 2\sigma(I)$]	$R_1 = 0.032$, $wR_2 = 0.086$	$R_1 = 0.039$, $wR_2 = 0.105$
R indices (all data)	$R_1 = 0.038$, $wR_2 = 0.091$	$R_1 = 0.059$, $wR_2 = 0.118$
Largest diff. peak and hole (e Å^{-3})	0.55 and −0.58	0.41 and −0.36

3.1.1. Crystal structure of [Ag(smz)(pyridine)] (1). The crystal structure of **1** consists of a silver, one sulfamethazine and one pyridine. Silver is four-coordinate from two sulfonamide nitrogens from two sulfamethazine ligands, one nitrogen from a pyridine ligand and another silver leading to a distorted tetrahedral geometry. The bond lengths involving silver represent a distorted tetrahedral configuration and are compatible to those (2.354–2.689 Å) reported in other silver complexes [28, 29]. The distance between silver and nitrogen adjacent to the sulfonyl group Ag–N1 = 2.195(2) Å is similar to previously reported distances in other Ag–N systems [30, 31]. A second bond involves the pyrimidine nitrogen of a symmetry-related ligand [Ag–N2^i = 2.204(2) Å], which is similar to silver sulfadiazine Ag–N distance [6, 7], while the third bond occurs along the lone electron pair of the nitrogen of pyridine [Ag–N5 = 2.469(3) Å]. The reported Ag–N (pyridine) distance for [$Ag_2(C_{10}H_{10}N_3O_3S)_2(C_5H_5N)_3$] is 2.403(7) Å [32]. The fourth bond due to each smz bridging two different silver ions [Ag–Ag^i = 2.7730(4) Å] is short compared to that in metallic silver (2.889 Å) and predicts metal–metal bonding involving s or d orbitals. The reported Ag···Ag separation for silver complex of sulfathiazole is 2.895(6) Å [30] and for silver sulfadiazine is 2.916(1) Å [6, 7].

The bond lengths and angles of the phenyl ring conform to those found in free sulfamethazine [11, 12], whereas distances [S1–N1 = 1.608(2) Å] and [N1–C7 = 1.374(3) Å] are shorter in the silver complex than those in free ligand [11, 12]. The stereochemistry about sulfur is a slightly distorted tetrahedral geometry with the bond lengths and angles involving sulfur lying within the range quoted in the literature [33–36]. The maximum and minimum value of angles around sulfur are 115.78(15)° [O1–S1–O2] and 103.55(12)°

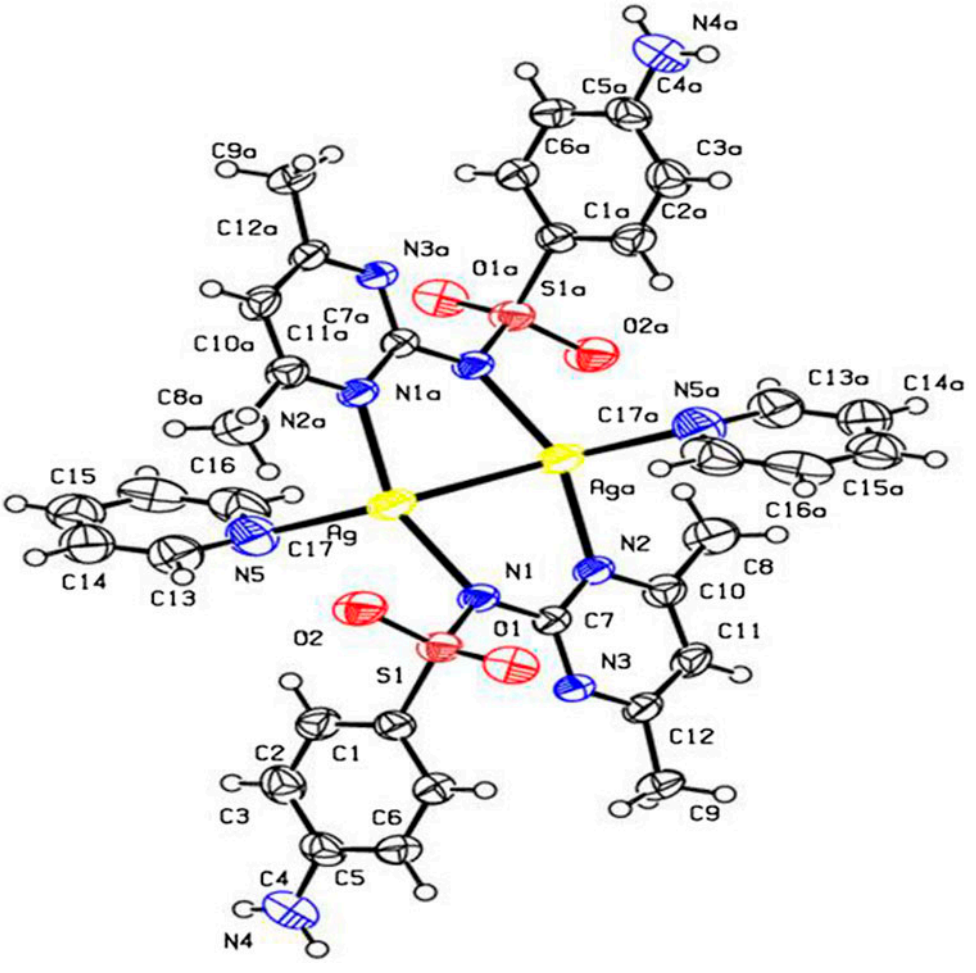

Figure 2. ORTEP diagram of [Ag(smz)(pyridine)] (**1**). Displacement ellipsoids are drawn at the 50% probability level.

[O2–S1–N1], respectively. The *gauche* conformation about the S–N (sulfonamidic) bond with a torsion angle of −62.3(2)° [C1–S1–N1–C7] is similar to that observed in silver sulfamethoxazole [32], but the angle is higher (−53.9°) in silver sulfadiazine [6]. The reported *gauche* conformation about the S–N (sulfonamidic) bond for free sulfamethazine has torsion angles of 83.2(3)° [11] and 84.2(6)° [12]. The phenyl ring is vertical to the pyrimidine ring with a dihedral angle of 81.35(1)°, while in free sulfamethazine, the angle is 75.5(1)° [11].

In the crystal structure, the molecules are linked via strong intermolecular and intramolecular interactions. Two of the intermolecular interactions are N–H···O hydrogen bonds formed by the terminal amino nitrogen and sulfonyl oxygen, one N–H···S hydrogen bond formed by the terminal amino nitrogen and sulfur, and one C–H···N hydrogen bond formed by methyl carbon and pyrimidine nitrogen of sulfamethazine. The intramolecualar C–H···O interaction is formed between phenyl ring carbon of sulfamethazine and the sulfonyl oxygen. The crystal structure exhibits C(9)–H(9B)···Cg(3) interaction [where Cg(3) is

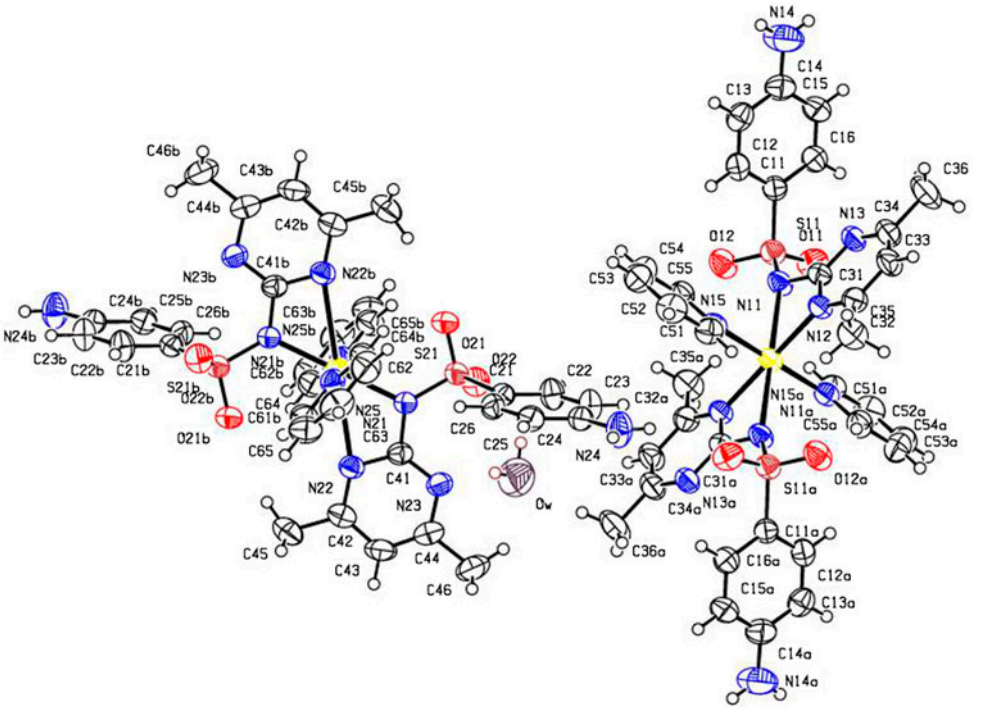

Figure 3. ORTEP diagram of $[Cu(smz)_2(pyridine)_2]\cdot H_2O$ (**2**). Displacement ellipsoids are drawn at the 50% probability level.

the centroid of the ring N2/N3/C7/C10/C11/C12 with a symmetry code $-x, 1-y, -z$], with a C–Cg distance of 3.3822 Å and C–H···*Cg* angle of 124°. The packing diagram of [Ag(smz)(pyridine)] (**1**) with N–H···O hydrogen bond interactions is presented in Supplemental data (figure S1, see online supplemental material at http://dx.doi.org/10.1080/00958972.2015.1055258).

3.1.2. Crystal structure of $[Cu(smz)_2(pyridine)_2]\cdot H_2O$ (2). The crystal structure of **2** contains two molecules per asymmetric unit cell with one crystalline water. Crystal structure of $[Cu(smz)_2(pyridine)_2]\cdot H_2O$ (**2**) consists of six-coordinate copper leading to a distorted octahedral geometry by two sulfonamidic nitrogens and two pyrimidine nitrogens from two sulfamethazine ligands and two pyridine ligands. The distance between copper and nitrogen adjacent to the sulfonyl group for the first molecule [Cu1–N11 = Cu1–N11^{i} = 2.4769(18) Å] and for the second molecule [Cu2–N21 = Cu2–N21^{i} = 2.0280(18) Å] are similar to previously reported distances in other Cu–N systems [37, 38]. Third and fourth bonds involve the pyrimidine nitrogens for the first molecule [Cu1–N12 = Cu1–N12^{i} = 2.0076 (19) Å] and for the second molecule [Cu2–N22 = Cu2–N22^{i} = 2.629(19) Å], which are similar to those reported for copper complexes of sulfamethazine [18, 19]. Fifth and sixth bonds involve the pyridine nitrogens for the first molecule [Cu1–N15 = Cu1–N15^{i} = 2.055 (2) Å] and for the second molecule [Cu2–N25 = Cu2–N25^{i} = 2.017(2) Å].

The bond lengths and angles of the phenyl ring conform well to those found in the free sulfamethazine [11, 12], whereas distances S1–N1(1.5980(19)) Å for the first molecule and

Table 2. Selected bond lengths and angles for **1** and **2**.

Bond lengths		Bond angles	
1			
Ag–N1	2.195(2)	N1–Ag–N2^{i}	154.78(8)
Ag–N2^{i}	2.204(2)	N1–Ag–N5	108.29(9)
Ag–N5	2.469(3)	N2^{i}–Ag–N5	96.88(10)
Ag–Ag^{i}	2.7730(4)	N1–Ag–Ag^{i}	78.80(5)
N2–Ag^{i}	2.204(2)	N2^{i}–Ag–Ag^{i}	85.80(5)
		N5–Ag–Ag^{i}	124.53(7)
		C7–N1–Ag	128.55(17)
		S1–N1–Ag	111.15(11)
		C10–N2–Ag^{i}	120.65(17)
		C7–N2–Ag^{i}	121.67(16)
		C13–N5–Ag	117.6(3)
		C17–N5–Ag	119.8(2)
2			
Cu1–N12^{i}	2.0076(19)	N12^{i}–Cu1–N12	180.00(12)
Cu1–N12	2.0076(19)	N12^{i}–Cu1–N15^{i}	91.94(8)
Cu1–N15^{i}	2.055(2)	N12–Cu1–N15^{i}	88.06(8)
Cu1–N15	2.055(2)	N12^{i}–Cu1–N15	88.06(8)
Cu1–N11^{i}	2.4769(18)	N12–Cu1–N15	91.94(8)
Cu1–N11	2.4769(18)	N15^{i}–Cu1–N15	180.0
Cu2–N25	2.017(2)	N12^{i}–Cu1–N11^{i}	59.50(7)
Cu2–N25^{i}	2.017(2)	N12–Cu1–N11^{i}	120.50(7)
Cu2–N21	2.0280(18)	N15^{i}–Cu1–N11^{i}	89.16(7)
Cu2–N21^{ii}	2.0280(18)	N15–Cu1–N11^{i}	90.84(7)
		N12^{i}–Cu1–N11	120.50(7)
		N12–Cu1–N11	59.50(7)
		N15^{i}–Cu1–N11	90.84(7)
		N15–Cu1–N11	89.16(7)
		N11^{i}–Cu1–N11	180.0
		N25–Cu2–N25^{ii}	180.00(12)
		N25–Cu2–N21	87.71(8)
		N25^{ii}–Cu2–N21	92.29(8)
		N25–Cu2–N21^{ii}	92.29(8)
		N25^{ii}–Cu2–N21^{ii}	87.71(8)
		N21–Cu2–N21^{ii}	180.0

Symmetry codes: **1** (i) $-x, -y, -z$; **2** (i) $-x, -y, -z+1$; (ii) $-x-1, -y-1, -z$.

1.5996(19) Å for the second molecule) and N11–C31 (1.364(3)) Å for the first molecule and 1.377(3) Å for the second molecule) are shorter in the copper complex than those in free sulfamethazine [11, 12]. The stereochemistry about sulfur is a slightly distorted tetrahedral geometry with the bond lengths and angles involving sulfur lying within the range quoted in the literature [33–35]. The trigonal arrangement around the sulfonamidic nitrogen is similar to those observed in Zn(II) and Cu(II)–sulfadiazine complexes [35]. The maximum and minimum value of angles around sulfur are for O12–S11–O11 (115.64(13)˚ for the first molecule and 115.32(11)˚ for the second molecule) and O12–S11–N11 (105.84 (10)˚ for the first molecule and 104.19(10)˚ for the second molecule). The *gauche* conformation about S–N (sulfonamidic) bond provides a torsion angle of 52.9(2)° [C11–S11–N11–C31] for the first molecule and −61.1(2)° [C21–S21–N21–C41] for the second molecule, which are lower than the values for a *gauche* conformation about the S–N (sulfonamidic) bond reported for the zinc sulfadiazine complex (−75.4° and −74.0°) [9], the silver sulfadiazine complex (−53.9°) [6], and free sulfamethazine (83.2(3)° [11] and 84.2(6)° [12]). The phenyl ring is nearly perpendicular to the pyrimidine ring showing a dihedral

Table 3. Hydrogen bond geometry for **1** and **2**.

D–H···A	D–H (Å)	D···A (Å)	H···A (Å)	∠D–H···A (°)
1				
N4–H4A···O2[a]	0.86	3.047(4)	2.47	126
N4–H4B···S1[b]	0.86	3.840(3)	3.00	167
N4–H4B···O2[b]	0.86	3.305(4)	2.54	149
C9–H9B···N3[c]	0.96	3.402(4)	2.68	132
C6–H6···O1	0.93	2.908(4)	2.52	105
2				
OW–HW1···N23[d]	0.97	3.083(4)	2.14	163
N14–H14A···O22[e]	0.86	3.043(4)	2.19	171
N14–H14B···OW	0.86	2.998(4)	2.49	119
N24–H24A···O11[f]	0.86	3.037(3)	2.24	154
N24–H24B···O11[g]	0.86	2.970(3)	2.13	166
C15–H15···O21[e]	0.93	3.418(3)	2.52	162
C16–H16···O11	0.93	2.912(4)	2.53	105
C45–H45A···O21[h]	0.96	3.431(4)	2.49	168
C65–H65···O21[h]	0.93	3.312(3)	2.56	138

Symmetry codes: [a]$-x+1, y-1/2, -z+1/2$; [b]$x, -y-1/2, z+1/2$; [c]$-x, -y-1, -z$; [d]$-x-2, -y-1, -z$; [e]$x, y+1, z$; [f]$x-1, y-1, z$; [g]$-x-1, -y, -z+1$; [h]$-x-1, -y-1, -z$.

angle of 86.74(16)° for the first molecule and 75.71(14)° for the second molecule, while in free sulfamethazine, the angle is 75.5(1)° [11].

In the crystal structure, the molecular stability is due to strong intermolecular and intramolecular interactions. Three of the intermolecular interactions are N–H···O hydrogen bonds formed by the terminal amino nitrogen and sulfonyl oxygen, one C–H···O hydrogen bond formed by the phenyl ring carbon of sulfamethazine and the sulfonyl oxygen and one O–H···N hydrogen bond formed between oxygen of water and pyrimidine nitrogen of sulfamethazine. Another two C–H···O hydrogen bond interactions are formed by the methoxy carbon of sulfamethazine and the sulfonyl oxygen and between pyridine ring carbon and sulfonyl oxygen. The intramolecualar N–H···O interaction is formed between the terminal amino nitrogen and water oxygen, where oxygen of water acts as an acceptor. One intramolecular C–H···O hydrogen bond is formed by the phenyl ring carbon of sulfamethazine and the sulfonyl oxygen. The crystal structure exhibits C(35)–H(35C)···Cg(8) interaction [where Cg(8) is the centroid of the ring N22/N23/C41/C42/C43/C44 with a symmetry code $x, y, 1+z$], with a C–Cg distance of 3.557(4) Å and C–H···Cg angle of 137°. The packing diagram of $[Cu(smz)_2(pyridine)_2]\cdot H_2O$ (**2**) with N–H···O hydrogen bond interaction is presented in Supplemental data (figure S2).

3.2. *IR spectra*

IR spectra of **1** and **2** from 4000 to 400 cm^{-1} are compared to the free ligand. Based on general references [39–41] and previous studies of complexes with sulfonamides [41–44], a tentative assignment of some important bands are listed in table 4. The bands between 3500 and 3400 cm^{-1} due to ν_{asym} (NH_2) and ν_{sym} (NH_2) of the amino ($-NH_2$) group are modified with respect to the free sulfamethazine. These modifications are probably due to the hydrogen bonding between complexes involving the NH_2 and SO_2 groups.

The peak for the sulfonamidic (N–H) group in the free ligand at 3093 cm^{-1} is not present in spectra of the complexes, confirming deprotonation of the $–SO_2NH–$ moiety. The scissoring vibrations for the amino ($–NH_2$) groups appear at 1639–1644 cm^{-1} and peaks due to

Table 4. Characteristic IR bands (cm^{-1}) of sulfamethazine, **1** and **2**.

Assignment	smz	**1**	**2**
ν_{as} (NH_2)	3442m	3425	3430
ν_s (NH_2)	3343s	3358	3280
ν (NH)amido	3240m	3245	3233
δ (NH_2)	1640	1639	1644
ν-phenyl ring	1596 and 1548	1598 and 1556	1597 and 1557
ν-pyrimidine ring	1428	1416	1433
$(SO_2)_{as}$	1325 and 1303	1377 and 1343	1371 and 1346
$(SO_2)_{sy}$	1146	1138	1141
δ (CH)phenyl	1091	1077	1075
ν (S–N)	1004 and 972	1012 and 979	1014 and 983

phenyl ring are at 1548 and 1598 cm^{-1}. The peaks at 1303 and 1377 cm^{-1} assigned to ν_{asym} (SO_2) and those at 1138–1146 cm^{-1} to ν_{sym} (SO_2) show significant changes upon complexation.

The 945–975 cm^{-1} band in the ligand is assigned to ν (S–N) [35, 45] at higher frequencies (958–1014 cm^{-1}) in both cases, as a consequence of coordination. These shifts to higher frequencies are in accord with the shortening of the S–N bond lengths which have been observed in the respective crystal structures of complexes.

3.3. *^{1}H NMR spectra*

Because the complexes are insoluble in less-polar solvents, their ^{1}H NMR spectra were recorded in a d_6-DMSO solution. The chemical shifts are expressed in ppm relative to internal TMS. The ^{1}H NMR data for **1** and **2** are presented in tables 5 and 6, respectively. From

Table 5. ^{1}H NMR chemical shifts (ppm) and assignment of sulfamethazine (smz) and **1** in DMSO-d_6[a].

Assignment	$^1H_{(smz)}$	$^1H_{(Ag–smz)}$	$\Delta\delta$ (H)[b]
N(1)–H	10.90	Absent	
C(11)–H	6.74	6.66	−0.08
C(2)–H/C(6)–H	7.68	7.68	0.00
C(3)–H/C(5)–H	6.59	6.51	−0.08
NH_2	5.95	5.65	−0.30
CH_3	2.28	2.50	+0.22

[a]Relative to TMS with DMSO-d_6 peak as reference (^{1}H, 2.60 ppm).
[b]$\Delta\delta = \delta$ (sulfonamide complex) − δ (sulfonamide).

Table 6. ^{1}H NMR chemical shifts (ppm) and assignment of sulfamethazine (smz) and **2** in DMSO-d_6[a].

Assignment	$^1H_{(smz)}$	$^1H_{(Cu-smz)}$	$\Delta\delta$ (H)[b]
N(11)–H	10.90	Absent	
C(33)–H	6.74	6.55	−0.19
C(12)–H/C(16)–H	7.68	7.63	−0.05
C(13)–H/C(15)–H	6.59	6.55	−0.04
NH_2	5.95	5.95	0.00
CH_3	2.28	2.25	−0.03

[a]Relative to TMS with DMSO-d_6 peak as reference (^{1}H, 2.60 ppm).
[b]$\Delta\delta = \delta$ (sulfonamide complex) − δ (sulfonamide).

the data, the ligand in the complexes exhibits low shifts in comparison to the free ligand. The most notable feature is that the ^{1}H NMR spectrum of the sulfamethazine ligand shows a broad singlet at 10.90 ppm, which may be assigned to sulfonamide NH proton. From previous study [46], the ^{1}H NMR spectrum of the sulfamethoxydiazine shows a broad singlet at 11.01 ppm. The absence of this proton signal in the spectra of the Ag(I) and Cu(II) complexes indicates that the sulfonamide NH group is deprotonated upon complex formation [47].

3.4. *UV–vis spectra*

The UV–vis spectra of free sulfamethazine and its silver and copper complexes are recorded in DMSO solution and are shown in figure 4. The electronic spectra of smz consist of two bands at 289 nm assigned to $\pi \rightarrow \pi^*$ transition of the phenyl ring and at 341 nm assigned to $n \rightarrow \pi^*$ intraligand transitions of their methyl groups. The silver ion has vacant 5d orbitals and consequently ligand-to-metal (L → M) binding can take place by the acceptance of one pair of electrons from the donor nitrogen of the ligand. The same transition is observed for silver complex of sulfamethazine with ^{1}S spectroscopic term. No *d–d* transition is expected for silver complex [48]. Similarly, the electronic spectra of the copper complex of sulfamethazine show transitions which are slightly shifted to shorter wavelengths as a result of decrease in conjugation of the system after complexation. The absorbance bands for

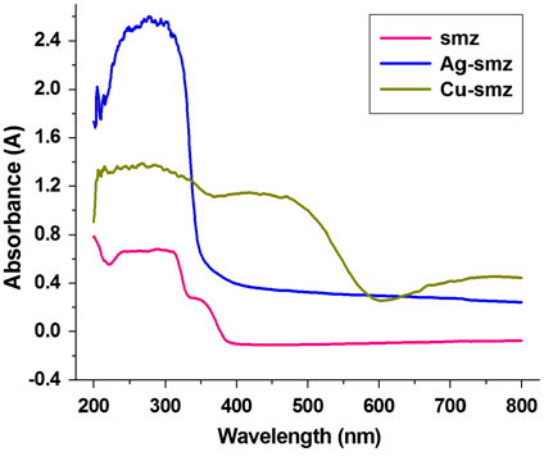

Figure 4. UV–vis spectra of DMSO solution of smz, **1** and **2**.

Table 7. Absorbance, wavelength, and assignment of sulfamethazine, **1** and **2**.

Compound	Wavelength (nm)	Energy (cm^{-1})	Assignment	Absorbance (A)
smz	289	34,602	$\pi \rightarrow \pi^*$	0.6825
	341	29,325	$n \rightarrow \pi^*$	0.2773
Ag-smz	278	35,971	$\pi \rightarrow \pi^*$	2.6014
Cu-smz	268	37,313	$\pi \rightarrow \pi^*$	1.3851
	418	23,923	LMCT	1.1457
	767	13,037	$^2E_g \rightarrow {}^2T_{2\,g}$	0.4545

Cu-smz were at 268 nm assigned to $\pi \rightarrow \pi^*$ transition, 418 nm to ligand-to-metal charge transfer transition (LMCT) and 767 nm assigned to *d–d* transition of a distorted octahedral copper(II) chromophore and attributed to $^2E_g \rightarrow {}^2T_{2g}$. The UV–vis bands of sulfamethazine (smz) and its silver and copper complexes are cited in table 7.

3.5. *TG analysis*

The silver and copper complexes of sulfamethazine and free smz are studied by TG analysis from ambient temperature to 967 °C in nitrogen atmosphere. The TGA curves are shown as % mass loss *versus* temperature, the differential thermogravimetric (DTG) curves are as the rate of loss of mass *versus* temperature. The thermal decomposition of **1** occurs with DTG

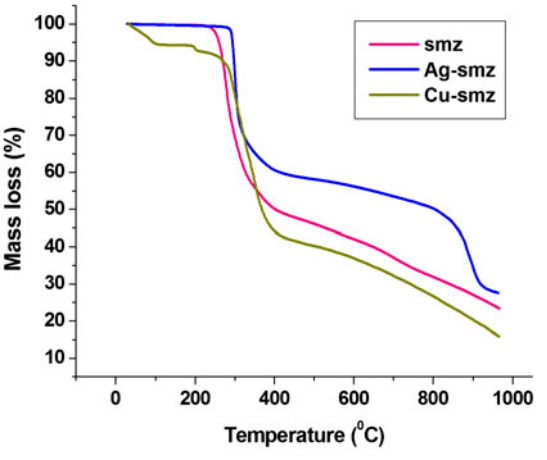

Figure 5. TGA curve of smz, **1** and **2**.

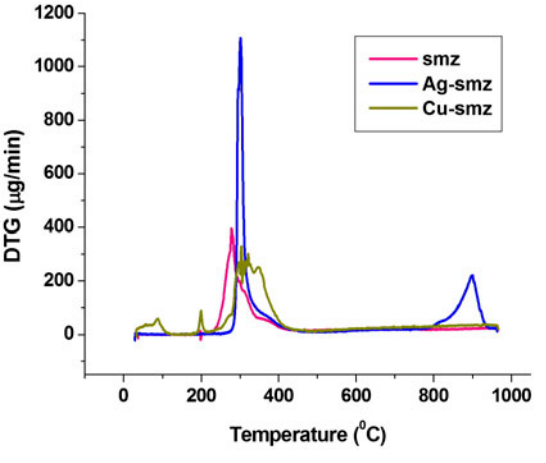

Figure 6. DTG curve of smz, **1** and **2**.

Table 8. Thermodynamic parameters of sulfamethazine and its silver and copper complexes.

Ligand/ Complex	Decomposition temperature range (K)	Activation energy (kJ mol^{-1})	Arrhenius constant	ΔH (kJ mol^{-1})	ΔS (J K^{-1} mol^{-1})	ΔG (kJ mol^{-1})
smz	541.91–559.92	144.64	30.13	140.06	−221.74	262.22
Ag-smz	571.36–578.41	321.59	65.87	316.81	−215.58	440.74
	1168.31–1175.34	224.46	23.86	214.72	−229.95	484.18
Cu-smz	352.03–369.22	26.07	5.75	23.07	−231.97	106.69
	462.46–480.88	26.96	4.35	23.04	−236.52	134.60
	567.84–585.77	75.35	14.45	70.56	−228.22	202.17

curve maxima showing endothermic peak at 301.84 °C (ΔH = 316.81 kJ mol^{-1}) and 898.81 °C (ΔH = 214.72 kJ mol^{-1}) and **2** occurs with DTG curve maxima showing endothermic peak at 87.45 °C (ΔH = 23.07 kJ mol^{-1}), 198.70 °C (ΔH = 23.04 kJ mol^{-1}), and 303.69 °C (ΔH = 70.56 kJ mol^{-1}), while in free sulfamethazine, an endothermic peak at 277.93 °C (ΔH = 140.06 kJ mol^{-1}) is observed. The final residual mass left at 963 °C is up to 27.57% for **1** and 16.07% for **2,** while in free smz, is 23.54%. The TG and DTG curves for free sulfamethazine (smz) and its silver and copper complexes are shown in figures 5 and 6, respectively. Thermodynamic parameters of both the synthesized complexes (**1**) and (**2**) of sulfamethazine and ligand (smz) itself have been evaluated by Broido's graphical method [49] for straight line decomposition portion of the thermodynamic analytical curve. Activation Energy (E_a) is calculated by the slope of ln(ln1/y) versus 1/T, where y is the fraction of the number of initial molecules not yet decomposed. The thermodynamic parameters like change in enthalpy (ΔH), entropy (ΔS), Gibb's free energy (ΔG), and Arrhenius constant (A) are calculated using the standard equations [50,51] and the data are presented in table 8.

3.6. *Microbiological assays*

The MIC values of sulfamethazine, **1** and **2** exhibited varying inhibitory effect against *S. aureus* and *E. coli* strains are tabulated in table 9. Complex **1** is sensitive towards gram negative bacteria (*E. coli*), while **2** is sensitive towards both gram positive bacteria (*S. aureus*) and gram negative bacteria (*E. coli*). According to the literature [52], the reported MIC values of silver sulfadoxine and silver sulfacetamide are 100 and 50 μg mL^{-1} towards gram positive bacteria (*S. aureus*), while toward gram negative bacteria (*Pseudomonas aurigi-nosa*), are 50 and 40 μg mL^{-1}. In the present study, the MIC value of silver complex of sulfamethazine is 100 μg mL^{-1} for *E. coli* strain, while 250 μg mL^{-1} for *S. aureus* strain. The results indicate *E. coli* strain is more sensitive for silver complex compared to *S. aureus* strain which is analogous to the reported data [53]. Additionally, the MIC values of Cu-smz

Table 9. MIC value (μg mL^{-1}) of sulfamethazine and its silver and copper complexes.

Compound	*Escherichia coli* MTCC 442	*Staphylococcus aureus* MTCC 96
smz	250	250
Ag-smz	100	250
Cu-smz	125	200
DMSO (control)	Nil	Nil

are 125 μg mL^{-1} for *E. coli* strain and 200 μg mL^{-1} for *S. aureus* strain. The results show that the biological activity screening of Cu-smz for both *E. coli* and *S. aureus* strain is higher compared to free sulfamethazine, which is similar to the other copper complexes of sulfonamides [54].

Our observations reveal that the MIC values for silver and copper complexes change according to the target bacteria. Gram positive bacteria (*S. aureus*) and gram negative bacteria (*E. coli*) have different cell wall constitution. *E. coli* have an outer lipidic membrane layer, while *S. aureus* do not.

4. Conclusion

Silver and copper complexes of sulfamethazine, **1** and **2** are synthesized, characterized, and tested as antimicrobial agents. Single crystals of silver and copper complexes of sulfamethazine are grown from pyridine solution by slow evaporation. The spectroscopic data are in agreement with the crystal structures. X-ray crystal structure analysis reveals distorted tetrahedral geometry for **1** and highly distorted octahedral geometry for **2**. Both **1** and **2** exhibit higher antibacterial activity than free sulfamethazine against gram negative bacteria.

Supplementary material

Full crystallographic data for the structures reported in this article have been deposited in the Cambridge Crystallographic Data Center for **1** and **2**, CCDC Nos. 1005649 and 1007751. Copies of this information can be obtained, free of charge, on application to CCDC, 12 Union Road, Cambridge, CB2 1EZ, U.K. (Fax: +44 1223 336033; or Email: deposit@ccdc.cam.ac.uk).

Acknowledgements

We are thankful to DST-FIST, New Delhi for funding towards the single-crystal diffractometer facility at Department of Physics, Sardar Patel University, Vallabh Vidyanagar. One of the authors (SMT) is thankful to UGC for RFSMS fellowship. The authors are thankful to Central Salt and Marine Chemicals Research Institute, CSMCRI, Bhavnagar for NMR, UV–vis spectra, and TGA data. We also acknowledge the help received from SICART, Vallabh Vidyanagar for CHN and IR data.

Disclosure statement

No potential conflict of interest was reported by the authors.

Funding

This work was supported by Department of Science and Technology, Ministry of Science and Technology, University Grants Committee, India.

References

[1] J.E. Toth, G.B. Grindey, W.J. Ehlhardt, J.E. Ray, G.B. Boder, J.R. Bewley, K.K. Klingerman, S.B. Gates, S.M. Rinzel, R.M. Schultz, L.C. Weir, J.F. Worzalla. *J. Med. Chem.*, **40**, 1018 (1997).
[2] J.C. Medina, D. Roche, B. Shan, R.M. Learned, W.P. Frankmoelle, D.L. Clark. *Bioorg. Med. Chem. Lett.*, **9**, 1843 (1999).
[3] H. Yoshino, N. Ueda, J. Niijima, H. Sugumi, Y. Kotake, N. Koyanagi, K. Yoshimatsu, M. Asada, T. Watanabe. *J. Med. Chem.*, **35**, 2496 (1992).
[4] T. Owa, H. Yoshino, T. Okauchi, K. Yoshimatsu, Y. Ozawa, N. Hata Sugi, T. Nagasu, N. Koyanagi, K. Kitoh. *J. Med. Chem.*, **42**, 3789 (1999).
[5] S. Roland, R. Ferone, R.J. Harvey, V.L. Styles, R.W. Morrison. *J. Biol. Chem.*, **254**, 10337 (1979).
[6] N.C. Baenziger, A.W. Struss. *Inorg. Chem.*, **15**, 1807 (1976).
[7] D.S. Cook, M.F. Turner. *J. Chem. Soc., Perkin Trans*, **2**, 1021 (1975).
[8] N.C. Baenziger, S.L. Modak, C.L. Fox Jr. *Acta Crystallogr., Sect. C*, **39**, 1620 (1983).
[9] C.J. Brown, D.S. Cook, L. Sengier. *Acta Crystallogr., Sect. C*, **41**, 718 (1985).
[10] F. de Zayas-Blanco, M.S. García-Falcón, J. Simal-Gándara. *Food Control*, **15**, 375 (2004).
[11] A.K. Basak, S.K. Mazumdar, S. Chaudhuri. *Acta Crystallogr., Sect. C*, **39**, 492 (1983).
[12] R.K. Tiwari, M. Haridas, T.P. Singh. *Acta Crystallogr., Sect. C*, **40**, 655 (1984).
[13] A. Bult, H. Sigel (Eds.). *Metal Ions in Biological Systems*, Vol. 16, Marcel Dekker, New York (1983).
[14] J.E.F. Reynolds (Ed.). *Martindale, The Extra Pharmacopoeia*, Royal Pharmaceutical Society, London (1996).
[15] E. Kremer, G. Facchin, E. Estévez, P. Alborés, E.J. Baran, J. Ellena, M.H. Torre. *J. Inorg. Biochem.*, **100**, 1167 (2006).
[16] J. Casanova, G. Alzuet, J. Borrás, J. Timoneda, S. García-Granda, I. Cándano-González. *J. Inorg. Biochem.*, **56**, 65 (1994).
[17] Z.H. Chohan, K. Mahmood-ul-Hassan, K.M. Khan, C.T. Supuran. *J. Enzyme Inhib. Med. Chem.*, **20**, 183 (2005).
[18] L. Gutiérrez, G. Alzuet, J. Borrás, A. Castiñeiras, A. Rodríguez-Fortea, E. Ruiz. *Inorg. Chem.*, **40**, 3089 (2001).
[19] J.B. Tommasino, F.N.R. Renaud, D. Luneau, G. Pilet. *Polyhedron*, **30**, 1663 (2011).
[20] Á. García-Raso, J.J. Fiol, S. Rigo, A. López-López, E. Molins, E. Espinosa, E. Borrás, G. Alzuet, J. Borrás, A. Castiñeiras. *Polyhedron*, **19**, 991 (2000).
[21] G.M. Golzar Hossain, A.J. Amoroso, A. Banu, K.M.A. Malik. *Polyhedron*, 26, 967 (2007).
[22] G.M. Sheldrick. *SHELXS2013: Program for Crystal Structure Solution*, University of Göttingen, Germany (2013).
[23] G.M. Sheldrick. *SHELXL2013: Program for Crystal Structure Refinement*, University of Göttingen, Germany (2013).
[24] A.L. Spek. *PLATON: A Multipurpose Crystallographic Tool*, Utrecht University, Utrecht, The Netherlands (2003).
[25] L.J. Farrugia. *J. Appl. Crystallogr.*, **30**, 565 (1997).
[26] L.J. Farrugia. *J. Appl. Crystallogr.*, **32**, 837 (1999).
[27] National Committee for Clinical Laboratory Standards. *Methods for Dilution Antimicrobial Susceptibility Tests for Bacteria that Grow Aerobically Approved Standard, M7A5*, 5th Edn, National Committee for Clinical Laboratory Standards, Wayne, PA (2000).
[28] M.A. Withersby, A.J. Blake, N.R. Champness, P. Hubberstey, W.-S. Li, M. Schröder. *Angew. Chem. Int. Ed. Engl.*, **36**, 2327 (1997).
[29] D.M. Ho, R. Bau. *Inorg. Chem.*, **22**, 4073 (1983).
[30] J.H. Bormio Nunes, R.E.F. de Paiva, A. Cuin, W.R. Lustri, P.P. Corbi. *Polyhedron*, **85**, 437 (2015).
[31] L.L. Marques, G. Manzoni de Oliveira, E. Schulz Lang, M.M. Anraku de Campos, L.R. Soccol Gris. *Inorg. Chem. Commun.*, **10**, 1083 (2007).
[32] S.M. Tailor, U.H. Patel. *J. Mol. Struct.*, **1088**, 161 (2015).
[33] U.H. Patel, S.A. Gandhi. *Indian J. Pure Appl. Phys.*, **49**, 263 (2011).
[34] U.H. Patel, B.H. Patel, B.N. Patel. *Cryst. Res. Technol.*, **36**, 1445 (2001).
[35] A. Garci´a-Raso, J.J. Fiol, G. Martorell, A. Lo´pez-Zafra, M. Quiro´s. *Polyhedron*, **16**, 613 (1997).
[36] A. Bult, N. Hulsing, J.N. Weyland. *J. Pharm. Pharmacol.*, **33**, 171 (1981).
[37] J. Ellena, E. Kremer, G. Facchin, E.J. Baran, O.R. Nascimento, A.J. Costa-Filho, M.H. Torre. *Polyhedron*, **26**, 3277 (2007).
[38] M.H. Torre, G. Facchin, E. Kremer, E.E. Castellano, O.E. Piro, E.J. Baran. *J. Inorg. Biochem.*, **94**, 200 (2003).
[39] D. Lin-Vien, N.B. Colthup, W.G. Fately, J.G. Grasselli. *The Handbook of Infrared and Raman Characteristic Frequencies of Organic Molecules*, Academic Press, San Diego, CA (1991).
[40] K. Nakamoto. *Infrared and Raman Spectra of Inorganic and Coordination Compounds*, John Wiley & Sons, New York (1997).
[41] K. Nakanishi. *IR-Absorption Spectroscopy – Practical*, Holden-Day Inc., San Francisco, CA (1962).

[42] B. Macías, I. García, M.V. Villa, J. Borrás, A. Castiñeiras, F. Sanz. *Polyhedron*, **21**, 1229 (2002).
[43] F. Blasco, L. Perelló, J. Latorre, J. Borrás, S. Garciá-Granda. *J. Inorg. Biochem.*, **61**, 143 (1996).
[44] W.L. Driessen, P.H. van der Voort. *Inorg. Chim. Acta*, **21**, 217 (1977).
[45] J. Casanova, G. Alzuet, S. Ferrer, J. Borrás, S. García-Granda, E. Perez-Carreño. *J. Inorg. Biochem.*, **51**, 689 (1993).
[46] L. Yang, X. Yang, J. Liu, Y. Li, Q. Lou, Q. Liu. *J. Coord. Chem.*, **56**, 1131 (2003).
[47] G. Kanagaraj, G.N. Rao. *Synth. React. Inorg. Met.-Org. Chem.*, **22**, 559 (1992).
[48] A.D. Tella, J.A. Obaleye. *Bull. Chem. Soc. Ethiop.*, **25**, 371 (2011).
[49] K.R. Venugopala Reddy, J. Keshavayya, J. Seetharamappa. *Dyes Pigments*, **59**, 237 (2003).
[50] A. Broido. *J. Polym. Sci.*, **7**, 1761 (1969).
[51] A.W. Coats, J.P. Redfern. *Nature*, **201**, 68 (1964).
[52] R.A. Herole, V.S. Velingkar. *Int. J. Pharm. Chem.*, **2**, 45 (2011).
[53] M.I. Azócar, G. Gómez, P. Levín, M. Paez, H. Muñoz, N. Dinamarca. *J. Coord. Chem.*, **67**, 3840 (2014).
[54] S. Alyar, N. Özbek, N.O. İskeleli, N. Karacan. *Med. Chem. Res.*, **22**, 2051 (2013).